Steady Shear Response of Carbon Nanotube Networks Dispersed in Poly(ethylene oxide)

Tirtha Chatterjee[†] **and Ramanan Krishnamoorti***

Department of Chemical and Biomolecular Engineering, University of Houston, Houston, Texas 77204-4004

Received March 23, 2008; Revised Manuscript Received May 20, 2008

ABSTRACT: The response of fractal networks of dispersed single walled carbon nanotubes in poly(ethylene oxide) to continuous constant-rate shear flow is examined as functions of shear rate and nanotube concentration. The steady shear viscosity values are strong functions of shear rate and follow a power-law shear-thinning character, while the nanotube concentration dependence of the viscosity (at a fixed shear rate) is somewhat weaker than the scaling of the equilibrium modulus values. For dispersions with nanotube concentrations corresponding to the semidilute regime, the stress response to constant-rate continuous shear from rest demonstrates a stress maximum that decays to a steady value at long times. The stress maximum and steady shear behavior can be reconciled in terms of the changing structure at the mesoscale for the fractal networks. On the other hand, the transient development of the stress during the start-up experiments can be qualitatively reconciled in the context of a cluster dynamics model.

I. Introduction

Efficient dispersion of nanoparticles in polymer matrices can potentially lead to the development of advanced materials with unique properties and competitive manufacturing cost that are similar to the processing of the original polymers.[1–4] Single walled carbon nanotubes (SWNTs) with their remarkable set of intrinsic properties[1] are outstanding nanoparticles to incorporate in polymer nanocomposites.[3,5] Despite this promise, the successful dispersion of nanotubes has remained a significant challenge in the production of SWNT-based polymer nanocomposites.[4] To overcome this problem, nanotubes are dispersed either as chemically functionalized moieties[6] or with the aid of surfactants acting as compatibilizers.[7] In a well-dispersed nanocomposite, the large aspect ratio of the nanotubes and their short-range attraction lead to the formation of a solidlike material with a network structure at relatively low nanotube loading (the onset of which is referred to as the percolation threshold, p_c, in vol %, without necessarily satisfying all the criteria of percolation).[3] This network superstructure, along with the ability to transfer stress from the continuous polymer matrix to the nanotube network, is responsible for the significant improvement of the nanocomposite mechanical properties.[2] In fact, as has been demonstrated previously, for nanocomposites with nanoparticle loadings well in excess of the percolation threshold the fractal nanotube network dominates the linear viscoelastic response.[2,8]

More interestingly, under constant rate steady shear these nanocomposites demonstrate non-Newtonian behavior similar to a range of complex fluids such as emulsions, pastes, and slurries.[9] In particular, the shear stress (σ) response to a constant shear rate ($\dot{\gamma}$) demonstrates the presence of an yield stress (σ_y), and the system flows like a power law fluids beyond that stress. Nevertheless, the underlying length and time scales that determine the flow properties, beyond the yield stress, are yet to be fully understood. Further, an understanding of the network deformation as a function of the particle concentration and the shear rate will lead to a significant improvement in the processing of such nanocomposites.

Previous studies related to the rheology of nanotube suspensions have examined SWNT suspensions in aqueous[10] or superacid[11] media. In those studies the shear viscosities of the nanocomposites were measured as functions of shear rate and of nanotube loading and associated with either the intrinsic properties of the nanotubes at low concentrations or their collections as liquid crystalline domains at high concentrations. Recently, Hobbie and co-workers[8] explored the yield and flow behavior following yield for suspensions of multiwalled nanotubes (MWNTs) dispersed in a low-molecular-mass fluid (polyisobutylene (PIB)) at intermediate concentrations, where they form a fractal superstructure, under controlled strain and controlled stress conditions. Kharchenko and co-workers have reported the flow-induced properties of MWNTs network in polypropylene matrix where significant shear thinning and more importantly large and negative normal stress difference were observed.[12] The negative normal stress differences result in die-contraction properties and presumably arise from the large-scale deformation of the network and the local deformation of nanotubes under shear.

In the present study we report the nonlinear viscoelastic properties of networks of SWNTs[2,3] dispersed in poly(ethylene oxide) (PEO) under shear. For this system the geometrical percolation threshold (p_c) is found to be ∼0.09 vol % with an effective anisotropy (α) of the percolating members being ∼650.[13] Semidilute concentrations of the nanotubes, $3.0 \leq p/p_c \leq 8.0$, are selected for this work. The merit of this selection is to ensure a fully developed network (which does not occur for $p/p_c < 3$) while not exceeding the critical loading required for inherently nematic structure formation.[2,9] A representative optical microscopy image of the dispersion in the melt state of the polymer ($T = 80$ °C) is shown in Figure 1a and demonstrates a homogeneous dispersion primarily consisting of small aggregated clusters or flocs. The overall mass fractal dimension of the network is found to be 2.3 ± 0.2.[2] A small- and ultrasmall-angle neutron scattering study revealed at least a two-level structural hierarchy where inside the flocs individual or small nanotube bundles overlap each other to form a relatively dense mesh.[3] A schematic of the hierarchical network structure showing different length scales is presented in Figure 1b. With increasing nanotube loading, the network becomes denser and the mesh size (ζ) decreases following a scaling relation ($\zeta \sim (p - p_c)^{-0.35\pm0.04}$), but the average floc size (R) is found to be largely independent of the particle concentration and ∼4 μm. On the other hand, the total number of flocs (N) increases with

* To whom correspondence should be addressed.
[†] Current address: Materials Research Laboratory, University of California, Santa Barbara, CA 93106.

10.1021/ma800640w CCC: $40.75
Published on Web 06/18/2008

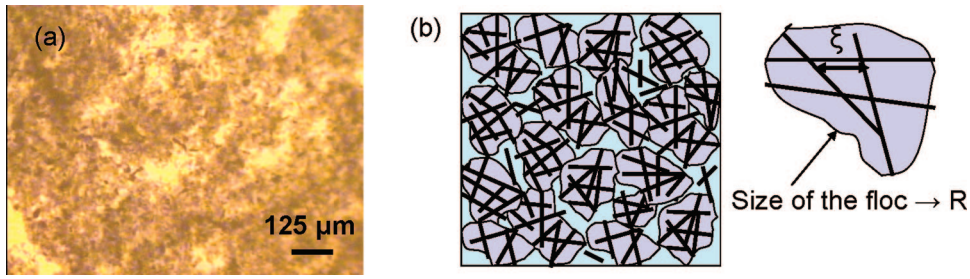

Figure 1. (a) Representative optical microscopy image of SWNTs dispersed in PEO matrix, obtained in the melt state of the polymer at $T = 80$ °C. The dark brown features correspond to the SWNTs flocs. In this sample, the SWNT concentration is ~8 times higher than the loading at percolation. (b) Schematic of the hierarchical network structure in quiescent state.[3] We note that the mesh and floc sizes (ζ and R, respectively) in the nanocomposites could be quite polydisperse.

nanotube concentration ($N \sim p^{1.1\pm0.1}$), indicating that with addition of nanotubes the network primarily grows through addition of new flocs.

The response of the fractal networks of SWNTs to steady shear is investigated as functions of shear rate and nanotube concentration and reported here. Specifically, we focus our attention on both the transient and steady-state response of the nanocomposites subjected to constant-rate shear flow. We understand these experimental findings in the context of cluster dynamics calculations and relate the dynamical properties to the established structure of these systems.

II. Materials and Methods

The nanocomposites used in this study were prepared using a surfactant-assisted dispersion technique.[13] The SWNTs (supplied by Carbon Nanotechnologies Inc.) were prepared by the HiPco process[14] and purified using standard techniques.[15] The polymer and surfactant were purchased from Aldrich Chemical Co. and used as received. The weight-average molecular weight (M_w) of poly(ethylene oxide) (PEO) was 8000 Da with a polydispersity (M_w/M_n) 1.14. The nanocomposites were compatibilized using lithium dodecyl sulfate, an anionic surfactant.[13] A detailed study of the state of dispersion of SWNTs in these nanocomposites has been reported previously.[13]

The macroscopic dispersion of SWNTs was characterized using an upright Nikon Optiphot-2 microscope in transmission mode. The microscope stage was attached to a temperature controller module, Linkam TMS 94. Samples at various SWNTs loadings were imaged above the melting point temperature of PEO matrix at 80 °C.

Melt-state ($T = 70$ °C) rheological measurements were performed on a TA Instruments ARES melt rheometer with a torque transducer range 0.2−2000 g_f cm and normal force range of 2−2000 g. For all samples, linear oscillatory and stress relaxation measurements were performed and results reported in a previous publication.[2] To understand the network behavior under flow, start-up of steady shear experiments were performed using cone-and-plate geometry with a plate diameter of 25 mm and a cone angle of ~0.1 rad. Compressive and biaxial strains that occur during the loading of the nanocomposite samples in the rheometer were kept as low as possible, and the sample was allowed to equilibrate for an extended period (24 h or longer) after loading and prior to testing. Samples were subjected to continuous shear ($0.05\ s^{-1} \le \dot{\gamma} \le 20\ s^{-1}$), applied until a steady value of all viscoelastic parameters were achieved. For shear rates lower than 0.05 s^{-1} the long time steady shear response is quite noisy, while for shear rate higher than 5 s^{-1} the instrument resolution fails to accurately record the initial transient response (short time data) but does provide reliable steady shear data (long time data). The detailed transient steady shear data analysis is performed for 2 decades of shear rate measurements ($0.05 \le \dot{\gamma} \le 5\ s^{-1}$) whereas for steady shear properties higher shear rates ($\dot{\gamma} > 5.0\ s^{-1}$) are also included.

For all the nanocomposite samples the steady shear measurements were started at the lowest shear rate and progressing to successively higher shear rates. Between two successive measurements a rest time ($t = 10\,000$ s) was imposed to allow the sample to recover. The length of the quiescent period was determined on the basis of flow reversal experiment, and little variance in rest time does not affect the steady shear measurements significantly as demonstrated in the Supporting Information. Further, to ensure the sufficiency of the given rest time, especially for high shear rate measurements, often a low shear rate measurement was repeated after execution of a high shear rate, and the reproducibility of the data with other shear histories was verified. For each shear rate the developed shear stress (σ) and the first normal stress difference N_{12} were monitored as a function of time.

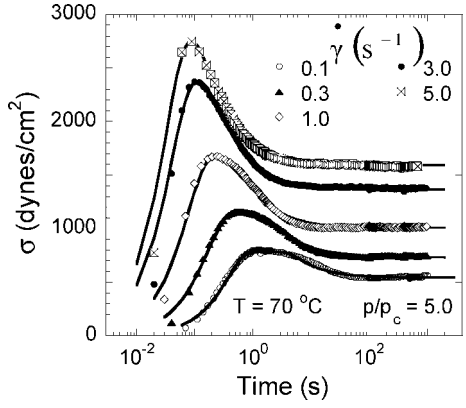

Figure 2. Transient shear stress response obtained during start-up of steady shear measurements for a SWNT-PEO dispersion with $p/p_c = 5.0$. For all shear rates, the stress data exhibit an initial overshoot arising from the shear-induced rearrangement of the cluster structure, and at long times the network reaches an equilibrium state to exhibit a steady viscoelastic response. Solid lines are model fit to the experimental data as described in eq 1.

III. Results and Discussion

The response to constant-rate steady shear is studied as a transient response from rest using start-up of steady shear measurements. Under continuous shear, the temporal development of the shear stress shows an initial stress overshoot that equilibrates to a well-defined steady state value (σ_∞) without any oscillations as seen in representative data in Figure 2. The stress overshoot behavior is attributed to the nanotube network superstructure. The parent polymer molecular weight is too low ($M_w/M_e \approx 3.6-5.0$, where M_e, the entanglement molecular weight, of PEO is 1600−2200)[16] for a chain entanglement effect to result in the stress overshoot. This feature is also absent in the steady shear response of nanocomposites with nanotube loading below the percolation threshold. The maximum of the stress overshoot is denoted as σ_{max}, and the time from start-up required to attain it is referred to as t_{peak}.

For a nanocomposite with nanotube concentration (p) above the percolation threshold (p_c) and with micron sized aggregate or flocs it would be expected that the relaxation behavior would

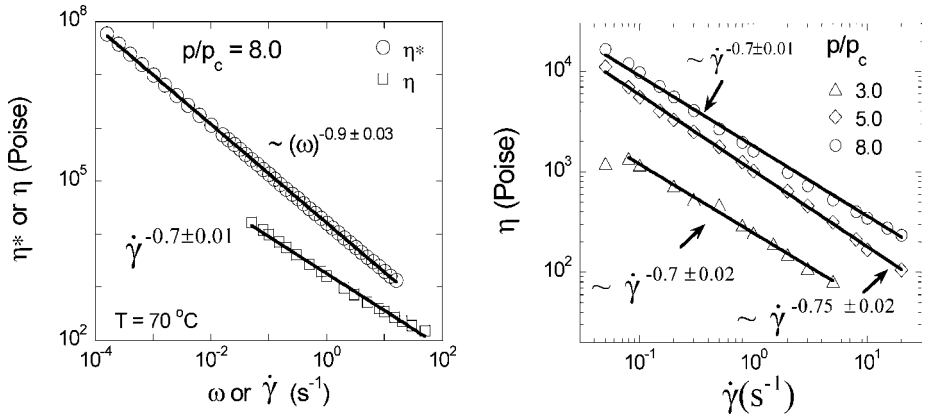

Figure 3. (a, left) Comparison of the steady shear viscosity with the complex viscosity of the nanocomposite. On the basis of the differences in the scaling of the viscosity with shear rate and frequency and the decreased absolute value of $\eta(\dot{\gamma})$ compared to $\eta^*(\omega=\dot{\gamma})$, we suggest that the mesoscale structure of the nanotube network alters as a result of the continuous constant-rate shear. (b, right) Shear-rate dependence of the steady shear viscosity for three nanocomposites, demonstrating the similarity of the power-law scaling for all three nanocomposites. Examining the nanotube concentration dependence of $\eta(\dot{\gamma})$ reveals a scaling of $\sim p^{2.5}$. We note that the concentration range over which we obtain such well-developed networks without the formation of liquid crystalline structures is limited to the range studied here.

be non-Brownian. Network formation along with the hierarchy of length scales and the inherent structural disorder that exist under quiescent or near-quiescent conditions in such a system render that thermal motion alone is insufficient to achieve complete structural relaxation. On the other hand, shear stresses imposed on such a material can result in structural rearrangements that dissipate the applied stress. A measure of the relative importance of the Brownian motion and shear-induced deformation is quantitatively given by the nondimensional Peclet number, and we consider two scenarios to estimate the Peclet number for the nanocomposites and verify that Brownian motion is not the dominant mode of structural relaxation for these materials. If the relaxation of the individual nanotubes is the primary mechanism for the relaxation process, then the rotational Peclet number (for slender rods, rotary diffusion is the dominant mode of relaxation) is given as $Pe = \dot{\gamma}/D_{rot,rod}$, where $D_{rot,rod}$ is the rotational diffusivity of the cylindrical nanotubes. For cylinders of length L and diameter d, the rotational diffusivity ($D_{rot,rod}$) is expressed as[17] $\pi\eta_0 L^3 D_{rot,rod}/3k_BT = \ln(\alpha) - 0.446$, where η_0 is the zero shear viscosity of the polymer matrix (20 P here) and k_BT is the Boltzmann factor. Using this rotary diffusivity and for $0.05\ s^{-1} \leq \dot{\gamma} \leq 20\ s^{-1}$, the associated Peclet number range is $1.0 < Pe < 415$. On the other hand, if the aggregated clusters of size (R) $\sim 4\ \mu$m are considered as the dominant objects responsible for the relaxation process, the rotational diffusivity is given as $D_{rot,sphere} = k_BT/8\pi\eta_0 R^3$ and $\sim 1.5 \times 10^{-6}\ s^{-1}$ and the associate Peclet numbers range from 3×10^4 to 1.3×10^7 for the nanocomposites described here. For both the cases considered here the $Pe > 1$, and thus we conclude that the measurements reported here are in the convective transport regime where it is expected that the shear rate controls the structures and the relaxation process of the network. Further in this regime, we expect no time-dependent oscillation in the transient shear and normal stresses as these are ascribed to tumbling and rotation of anisotropic particles in the Brownian regime.[9]

In Figure 3a we compare and contrast the steady shear viscosity ($\eta = \sigma_\infty/\dot{\gamma}$) with the complex viscosity (η^*) obtained from linear viscoelastic measurements using small-amplitude oscillatory shear for a representative nanocomposite.[2,13] At comparable values of frequency (ω) and shear rate ($\dot{\gamma}$), $\eta(\dot{\gamma})$ is always less than $\eta^*(\omega)$. Further, $\eta(\dot{\gamma})$ shows a weaker scaling with $\dot{\gamma}$ (i.e., $\eta \sim \dot{\gamma}^{-0.7\pm0.01}$) as compared to $\eta^*(\omega)$ with ω (i.e., $\eta^*(\omega) \sim \omega^{-0.9\pm0.03}$).

Similar behavior for the rate dependence of $\eta(\dot{\gamma})$ is observed for all the nanocomposites as seen in Figure 3b. Irrespective of the SWNT loading, the nanocomposites exhibit shear thinning character with roughly similar dependence on shear rate, i.e., $\eta \sim \dot{\gamma}^{-0.73\pm0.05}$, and weaker than the corresponding η^* scaling with ω (i.e., $\eta^*(\omega) \sim \omega^{-0.9}$). Examining the concentration dependence at a fixed value of ω of η^* indicates a scaling of $\sim p^{3.5}$. On the other hand, a similar analysis of η at a fixed value of $\dot{\gamma}$ suggests a scaling of $\sim p^{2.5}$ over the narrow range of concentrations used in this study. These three features, i.e., (i) lower absolute magnitude of η compared to η^* at comparable values of ω and $\dot{\gamma}$, (ii) the weaker dependence on shear rate for η as compared to η^*, and (iii) the weaker concentration scaling of η as compared to η^*, indicate that the application of continuous steady shear results in significant changes in the dissipation mechanism as compared to the quiescent or near-quiescent state structure that is dominated by the mass fractal based network of flocs or aggregates. On the basis of the weaker network (i.e., lower viscosity) and weaker scaling with nanotube concentration of the steady shear viscosity, it is clear that some of the network elements (or junctions) that bear stress are eliminated during the application of continuous shear. Because of the fact that these nanocomposites in fact do flow when subjected to continuous shear, it is conceivable that the network elements (present at quiescent conditions) that resist deformation in the flow direction are eliminated. Assuming an initial isotropic state under quiescent conditions, the network elements resisting the displacement along the flow direction would nominally constitute 1/3 of all elements and their elimination (from the stress-bearing function) would decrease the reinforcement by that factor. The nanotube concentration dependence for η and the same for η^* are certainly consistent with the elimination of stress-bearing network elements as is the frequency or shear rate dependence of the viscosity. It is conceivable that at extremely high frequencies, where the viscosity data from linear dynamic and steady shear measurements would potentially intersect, the viscosity and the rate dependence would be dominated by extremely local modes of stress dissipation and in fact expected to be considerably different from the case of network dominated behavior at low shear rates (or frequencies).

While it is clear that the nanotube network and its deformation in response to the applied continuous shear dominate the steady shear response, the stress overshoot observed in the transient data also emerges, at least qualitatively, from the percolated network structure of the dispersed nanotubes. It is particularly insightful to note that both σ_{max} and σ_∞ vary almost identically with $\dot{\gamma}$ (i.e., $\dot{\gamma}^{0.3}$). This is captured in Figure 4, where the normalized stress overshoot ($\sigma_{max}/\sigma_\infty$) is shown as a function

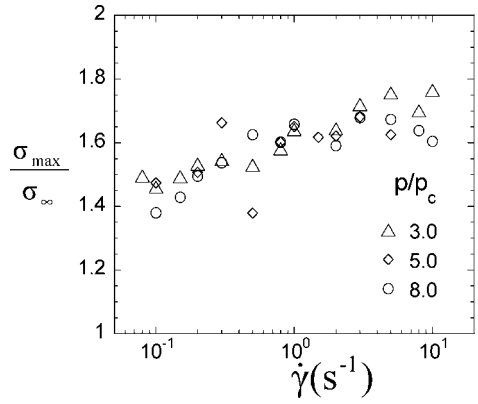

Figure 4. Under constant-rate continuous shear, the maximum shear stress (σ_{max}) and steady state shear stress (σ_∞) vary almost identically with $\dot{\gamma}$ (i.e., $\sim\dot{\gamma}^{0.3}$), leading to a near shear-rate-independent value of $\sigma_{max}/\sigma_\infty$. Moreover, the normalized stress overshoot (normalized by the steady stress value) is independent of the nanotube loading as well as the shear rate.

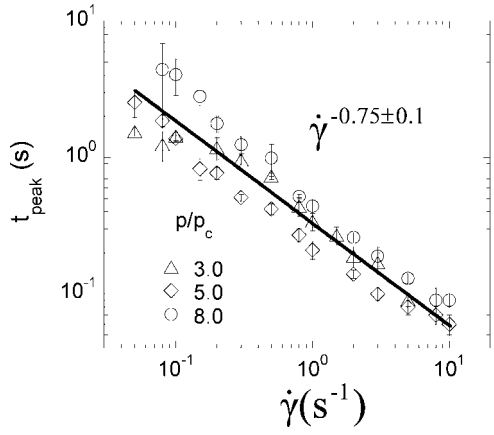

Figure 5. Time required to attain maximum stress (t_{peak}) by the network is independent of the nanotube loading and depends only on the shear rate. The value of t_{peak} does not scale with strain rate or the total strain.

of $\dot{\gamma}$. Clearly, two features are observed from these data: (a) $\sigma_{max}/\sigma_\infty$ is only weakly dependent on $\dot{\gamma}$ (scaling as $\dot{\gamma}^{0.03}$) and varying from 1.4 to 1.8 over the shear rates and nanotube loadings examined; (b) $\sigma_{max}/\sigma_\infty$ is largely independent of the nanotube loading. This observation suggests that the stress overshoots observed and the steady shear response are intimately related and perhaps a reflection of the structure of the nanocomposite as it evolves when subjected to continuous shear.

We next examine the shear rate and nanotube concentration effects on the location of the peak in the transient shear stress signal (Figure 5). The time of the stress maximum (t_{peak}) shows two features: (a) it is roughly independent of the nanotube concentration, and (b) it follows a power law dependence on the shear rate with a scaling exponent $-(0.75 \pm 0.1)$ (i.e., $t_{peak} \propto \dot{\gamma}^{-(0.75\pm0.10)}$). This power law scaling lies between those expected for Brownian moieties ($\dot{\gamma}^0$) and that for systems dominated by non-Brownian hydrodynamic stress controlled moieties ($t_{peak} \propto \dot{\gamma}^{-1}$).[9,20] While similar scaling behavior is observed in other nanocomposites, such as the case of dispersed grafted spherical silica nanoparticles in a polymer matrix,[18] in this case where the nanotube network dominates the viscoelastic response, we contend, as shown below, that that unique scaling is a result of competing mechanisms of the storage and dissipation of energy in such fractal networks. Our hypothesis, consistent with the findings of others, is that the peak in the shear stress originates the percolating network structure of nanoparticles.[18–20] This unique shear rate dependence of the t_{peak} is probably an outcome of the structure continuously evolving under steady shear and is discussed in detail below.

We have attempted to characterize the transient shear data by considering the effects of changing nanotube concentration and shear rate on the final steady stress and the characteristics of the peak in the transient stress data (i.e., the stress overshoot). We now consider the entire evolution of the shear stress when subjected to continuous constant rate shear from start-up. At short times after start-up, the material, behaving like a solid, would generate a stress that is roughly proportional to the total strain ($=\dot{\gamma}t$). On the other hand, the strain also induces structural rearrangement of the nanoparticle network, akin to a shear rejuvenation process, and these structural rearrangements and altered network structure would act to dissipate the stress generated or stored in the system. Whittle and Dickinson using Brownian dynamics have observed stress overshoot in model particle based gels and suggested a semiempirical model:[21]

$$\sigma(t) = \sigma_0 \frac{t/\tau_1}{1 + (t/\tau_1)^{1+\delta}} + \sigma_\infty \left\{ 1 - \exp\left(\frac{t}{\tau_2}\right) \right\} \qquad (1)$$

where τ_1 and τ_2 are the characteristic time scales associated with the rearrangement of the network structure under shear and the network break up (or flow), respectively, and δ is a phenomenological parameter. The parameter σ_0 is related to the shear-rate-dependent elastic modulus of the material, and σ_∞ is the steady state shear stress at the shear rate. For the shear rate range ($0.05\ s^{-1} \le \dot{\gamma} \le 5\ s^{-1}$), studied here, this model fits the experimental data quite well (solid lines in Figure 2) with exception of very short times. This discrepancy at short times is probably a consequence of the elastic deformation prediction by the model at very short time (for $t/\tau_1 \ll 1.0$, the evolved stress is given by $\sigma(t) = \sigma_0 t/\tau_1$). This does not represent the true structural state of the nanocomposites where simultaneous existence of mutually opposing structural rearrangement to bear the evolved stress and viscous dissipation mechanism may cause nonlinearity. As noted by Whittle and Dickinson, for times that are in the intermediate zone, i.e., $t > \tau_1$, the first term reduces to a power law decay process whose rate depends on the numerical value of δ. In our case, δ gradually increases with increasing shear rate from a value of 0.5 to a value of 1.4. This implies that with increasing shear rate the decay process becomes increasingly more important compared to the elastic response. On the other hand, the second term (exponential term) in eq 1 describes the long-time behavior and is related to the network relaxation process that leads to the steady flow (with an equilibrium number of stress-bearing members or contacts) with an equilibrium stress value (σ_∞) at long time.

In Figure 6, the characteristic times corresponding to the stress buildup (due to structural rearrangement) (τ_1) and to the stress dissipation (due to network flow) (τ_2) are presented as a function of shear rate for all the nanocomposites. The first most striking feature observed, similar to the observation for the peak time (t_{peak}), is the virtual independence of the quantitative values of τ_1 and τ_2 with nanotube concentration and reiterating the point made previously that the steady shear response is dominated by the deformation rate alone. Further, a quantitative comparison of τ_1 and τ_2 indicates that the characteristic time τ_2, corresponding to the stress dissipation, always exceeds the value of τ_1, corresponding to the structural rearrangement in these nanocomposites. This observation suggests that under continuous shear the fractal nanotube network first rearranges the structure to bear the evolved stress and beyond a threshold total strain of $\sim\dot{\gamma}t_{max}$ flows. Finally, a quantitative comparison of the shear rate dependence of the characteristic times τ_1 and τ_2 indicates that both characteristic times follow power-law scaling and with $\tau_1 \sim \dot{\gamma}^{-0.6\pm0.03}$and $\tau_2 \sim \dot{\gamma}^{-0.9\pm0.05}$ for the low and intermediate

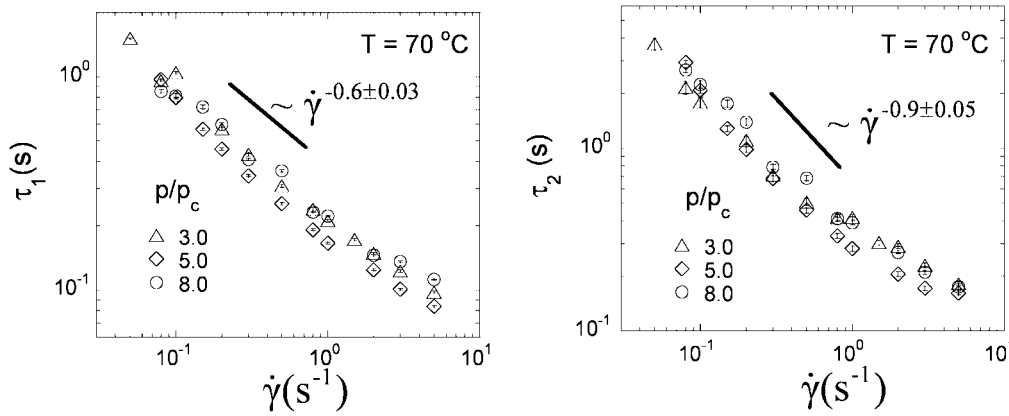

Figure 6. Model calculated characteristic times, described in eq 1, are shown as functions of shear rate and nanotube concentration. Both characteristic times show nanotube concentration-independent nature and depend only on the shear rate.

shear rates. For the highest shear rates these dependencies appear to become weaker; however, we were unable to pursue a rigorous study of this change due to instrumental limitations in sufficiently resolving the early time data.

We propose a simple physical picture which is consistent with the quiescent state SANS inferred structure[3] to reconcile the results described above. Under quiescent conditions, the fractal nanotube network, consisting of micron-sized flocs (which are roughly independent of nanotube concentration) and a relatively dense mesh within (that densifies slowly with increasing nanotube concentration), dominates the viscoelastic response and is largely elastic. We can readily eliminate any significant contribution from the polymer (either bulk or confined) due to the relatively low molecular weight of the chains (eliminating entanglements) and because the time scales examined are much longer than the longest relaxation time of the chains and the relatively low volume fraction of dispersed nanotubes (eliminating bridging and confinement induced slowdown of dynamics). Thus, we conjecture that the changes in the fractal network structure upon imposition of continuous shear (both shear-induced formation of stress-bearing bonds and shear-induced breakdown of stress-bearing contacts) are responsible for the observed transient and steady shear properties.

For dense colloidal suspensions under continuous strain, Silbert et al. found an inhomogeneous distribution of the stress with few high-stress bearing clusters and the population of such clusters essentially controls the stress response.[22] On the other hand, recent nonequilibrium molecular dynamics simulation studies of (high molecular weight) polymer nanocomposites have shown that the stress overshoot results from the elastic stretching of the particle−polymer network.[20] More importantly, they also found an inhomogeneity in stress distribution, and they found that only a small number of bonds actually carry the excess stress developed. These observations point toward understanding the steady shear behavior through a cluster dynamics argument.

We conjecture that under steady shear the flocs locally rearrange in response to the applied deformation and results in cluster−cluster collisions and jamming of the network elements that gives rise to the observed stress overshoot. With continuous shearing and when the local stress exceeds the yielding stress, the network bonds break and the network flows until a final steady state is reached where an equilibrium between bond formation and bond breaking occurs.[21] Considering the high viscosity of the system, the imposed shear is expected to set the time scale for cluster−cluster collisions. The collision frequency factor (k_{ij}) for fractal systems is given by[23] $k_{ij} = 2k_BT(R_i^{1/d_f} + R_j^{1/d_f})/3\eta(R_i^{1/d_f}R_j^{1/d_f})$, where R_i and R_j are the cluster sizes and d_f is the overall mass fractal dimension of the system. For concentration-independent cluster sizes,[3] the structural rearrangement time scale ($=1/k_{ij}$) is expected to show a shear rate scaling similar to that of the viscosity (η). Thus, in light of the similar dependencies of the shear rate dependencies of the viscosity (both the low-strain complex viscosity and steady shear viscosity), we expect and confirm experimentally that the characteristic time scale (τ_1) is only dependent on the applied shear rate and the power-law scaling of η and τ_1 are similar.

On the other hand, the process to a steady flowing behavior is governed by an establishment of equilibrium between bond-breaking and bond-formation processes. The Smoluchowski rate coefficient for the breakup process, g_n, scales with both shear rate and concentration as $g_n = 4\dot{\gamma}\phi/\pi$, where ϕ ($=p/100$) is the volume fraction of particles.[21,24] Thus, for a given nanocomposite, it is expected that the structural relaxation time (τ_2) scales inversely with the applied shear rate. Experimentally, we observe that for all the nancomposites $\tau_2 \sim \dot{\gamma}^{-0.9\pm0.05}$, in good agreement with this model. However, this Smoluchowski-type rate expression also requires that τ_2 scales with concentration of nanotubes, a feature notably absent in the experimental data. This disagreement might be caused by the properties of the shear-deformed structure that have not been probed by direct experiments and these are expected to control the breakup process. Alternatively, these differences may also result from inhomogenities in the stress and strain fields in such nanocomposites that might lead to a loss of the expected concentration dependence. Nonetheless, the above discussion indicates that the overall macroscopic steady shear response can be viewed in terms of cluster dynamics of the flocs present in such nanocomposites. Although the analysis presented here is largely qualitative, it provides an impetus toward a more detailed theoretical understanding of the system.

IV. Conclusions

The steady shear properties of isotropic dispersions of single walled carbon nanotubes in a poly(ethylene oxide) matrix in their semidilute concentration regime have been investigated here and understood in the context of cluster dynamics. Compared to the quiescent state structure and properties, the application of continuous shear at a fixed shear rate leads to significant changes in the rheological properties of the nanocomposites. We have conjectured that the most significant concentration and shear rate dependencies observed for both the transient and steady state properties can be reconciled in the context of the quiescent state structure and the application of shear-induced cluster dynamics on such a system. While this captures many of the aspects of the observed rheological behavior, some of the similarities of the observed rheological properties to highly entangled polymer melts and concentrated

solutions of highly entangled polymers are striking.[25] Perhaps the fractal-like behavior of the network elements (mesh level) and clusters and the hierarchy of structures allows for such a similarity. However, the non-Brownian nature of the nanotubes, nanotube aggregates, and flocs could explain, for instance, the observed intermediate scaling of the stress overshoot with shear rate, wherein it lies between the strain rate scaling and the total strain scaling, and significantly different from characteristic polymer behavior.

Acknowledgment. We gratefully acknowledge the support of the National Science Foundation (CMMI-0708096), AFOSR (FA9550-06-1-0422), and useful discussions with Prof. Shi-Qing Wang and Prof. Hiroshi Watanabe. We also thank Dr. Vijay Tirumala for useful discussions and help with the optical microscopy measurements.

Supporting Information Available: Experimental details, model fitting, and supplementary experimental evidence. This material is available free of charge via the Internet at http://pubs.acs.org.

References and Notes

(1) (a) Ajayan, P. M.; Charlier, J.-C.; Rinzler, A. G. *Proc. Natl. Acad. Sci.* **1999**, *96* (25), 14199–14200. (b) Ajayan, P. M.; Schadler, L. S.; Giannaris, C.; Rubio, A. *Adv. Mater.* **2000**, *12* (10), 750.
(2) Chatterjee, T.; Krishnamoorti, R. *Phys. Rev. E* **2007**, *75* (5), 050403.
(3) Chatterjee, T.; Jackson, A. J.; Krishnamoorti, R. *J. Am. Chem. Soc.* **2008**, *130*, 6934−6935.
(4) (a) Krishnamoorti, R. *MRS Bull.* **2007**, *32*, 341–347. (b) Chatterjee, T.; Mitchell, C. A.; Hadjiev, V. G.; Krishnamoorti, R. *Adv. Mater.* **2007**, *19*, 3850.
(5) Winey, K. I.; Vaia, R. A. *MRS Bull.* **2007**, *32* (4), 314–319.
(6) (a) Banerjee, S.; Hemraj-Benny, T.; Wong, S. S. *Adv. Mater.* **2005**, *17* (1), 17–29. Mitchell, C. A.; Bahr, J. L.; Arepalli, S.; Tour, J. M.; Krishnamoorti, R. *Macromolecules* **2002**, *35* (23), 8825–8830.
(7) (a) Gong, X. Y.; Liu, J.; Baskaran, S.; Voise, R. D.; Young, J. S. *Chem. Mater.* **2000**, *12*, 1049–1052. (b) Vaisman, L.; Wagner, H. D.; Marom, G. *Adv. Colloid Interface Sci.* **2006**, *128*, 37–46. (c) Yurekli, K.; Mitchell, C. A.; Krishnamoorti, R. *J. Am. Chem. Soc.* **2004**, *126*, 9902–9903. (d) Mitchell, C. A.; Krishnamoorti, R. *Macromolecules* **2007**, *40*, 1538–1545.
(8) (a) Hobbie, E. K.; Fry, D. J. *Phys. Rev. Lett.* **2006**, *97* (3), 036101. (b) Hobbie, E. K.; Fry, D. J. *J. Chem. Phys.* **2007**, *126* (12), 124907.
(9) Larson, R. G. *The Structure and Rheology of Complex Fluids*, 1st ed.; Oxford University Press: New York, 1999.
(10) Shaffer, M. S. P.; Windle, A. H. *Macromolecules* **1999**, *32* (20), 6864–6866.
(11) Davis, V. A.; Ericson, L. M.; Parra-Vasquez, A. N. G.; Fan, H.; Wang, Y. H.; Prieto, V.; Longoria, J. A.; Ramesh, S.; Saini, R. K.; Kittrell, C.; Billups, W. E.; Adams, W. W.; Hauge, R. H.; Smalley, R. E.; Pasquali, M. *Macromolecules* **2004**, *37* (1), 154–160.
(12) Kharchenko, S. B.; Douglas, J. F.; Obrzut, J.; Grulke, E. A.; Migler, K. B. *Nat. Mater.* **2004**, *3* (8), 564–568.
(13) Chatterjee, T.; Yurekli, K.; Hadjiev, V. G.; Krishnamoorti, R. *Adv. Funct. Mater.* **2005**, *15* (11), 1832–1838.
(14) Nikolaev, P.; Bronikowski, M. J.; Bradley, R. K.; Rohmund, F.; Colbert, D. T.; Smith, K. A.; Smalley, R. E. *Chem. Phys. Lett.* **1999**, *313* (1−2), 91–97.
(15) Chattopadhyay, D.; Galeska, L.; Papadimitrakopoulos, F. *J. Am. Chem. Soc.* **2003**, *125* (11), 3370–3375.
(16) Ferry, J. D. *Viscoelastic Properties of Polymer*; John Wiley & Sons: New York, 1980.
(17) (a) Broersma, S. *J. Chem. Phys.* **1960**, *32* (6), 1626–1631. (b) Broersma, S. *J. Chem. Phys.* **1981**, *74* (12), 6989–6990.
(18) Goel, V.; Chatterjee, T.; Bombalski, L.; Yurekli, K.; Matyjaszewski, K.; Krishnamoorti, R. *J. Polym. Sci., Part B: Polym. Phys.* **2006**, *44* (14), 2014–2023.
(19) Ren, J. X.; Krishnamoorti, R. *Macromolecules* **2003**, *36* (12), 4443–4451.
(20) Thomin, J. D.; Keblinski, P.; Kumar, S. K. Submitted to *Macromolecules*.
(21) Whittle, M.; Dickinson, E. *J. Chem. Phys.* **1997**, *107* (23), 10191–10200.
(22) Silbert, L. E.; Farr, R. S.; Melrose, J. R.; Ball, R. C. *J. Chem. Phys.* **1999**, *111* (10), 4780–4789.
(23) Axford, S. D. T. *Proc. R. Soc. London, Ser. A* **1996**, *452* (1953), 2355–2368.
(24) Axford, S. D. T. *J. Chem. Soc., Faraday Trans.* **1996**, *92* (13), 2503–2503.
(25) (a) Ravindranath, S.; Wang, S. Q.; Ofechnowicz, M.; Quirk, R. P. *Macromolecules* **2008**, *41* (7), 2663–2670. (b) Ravindranath, S.; Wang, S. Q. *Macromolecules* **2007**, *40* (22), 8031–8039.

MA800640W